

Chitosan-PVA-CNT nanofibers as electrically conductive scaffolds for cardiovascular tissue engineering

Shabnam Mombini, Javad Mohammadnejad, Behnaz Bakhshandeh, Asghar Narmani, Jhamak Nourmohammadi, Sadaf Vahdat, Shahrzad Zirak



PII: S0141-8130(19)33683-9

DOI: <https://doi.org/10.1016/j.ijbiomac.2019.08.046>

Reference: BIOMAC 13023

To appear in: *International Journal of Biological Macromolecules*

Received date: 18 May 2019

Revised date: 30 July 2019

Accepted date: 6 August 2019

Please cite this article as: S. Mombini, J. Mohammadnejad, B. Bakhshandeh, et al., Chitosan-PVA-CNT nanofibers as electrically conductive scaffolds for cardiovascular tissue engineering, *International Journal of Biological Macromolecules*(2019), <https://doi.org/10.1016/j.ijbiomac.2019.08.046>

This is a PDF file of an article that has undergone enhancements after acceptance, such as the addition of a cover page and metadata, and formatting for readability, but it is not yet the definitive version of record. This version will undergo additional copyediting, typesetting and review before it is published in its final form, but we are providing this version to give early visibility of the article. Please note that, during the production process, errors may be discovered which could affect the content, and all legal disclaimers that apply to the journal pertain.

Chitosan-PVA-CNT nanofibers as electrically conductive scaffolds for cardiovascular tissue engineering

Shabnam Mombini^a, Javad Mohammadnejad^{a*}, Behnaz Bakhshandeh^{b*}, Asghar Narmani^a, Jhamak Nourmohammadi^a, Sadaf Vahdat^b, Shahrzad Zirak^a

^a Department of Life Science Engineering, Faculty of New Sciences & Technologies, University of Tehran, P.O. Box: 14395-1561, Tehran, Iran.

^b Department of Biotechnology, College of Science, University of Tehran, Tehran, Iran.

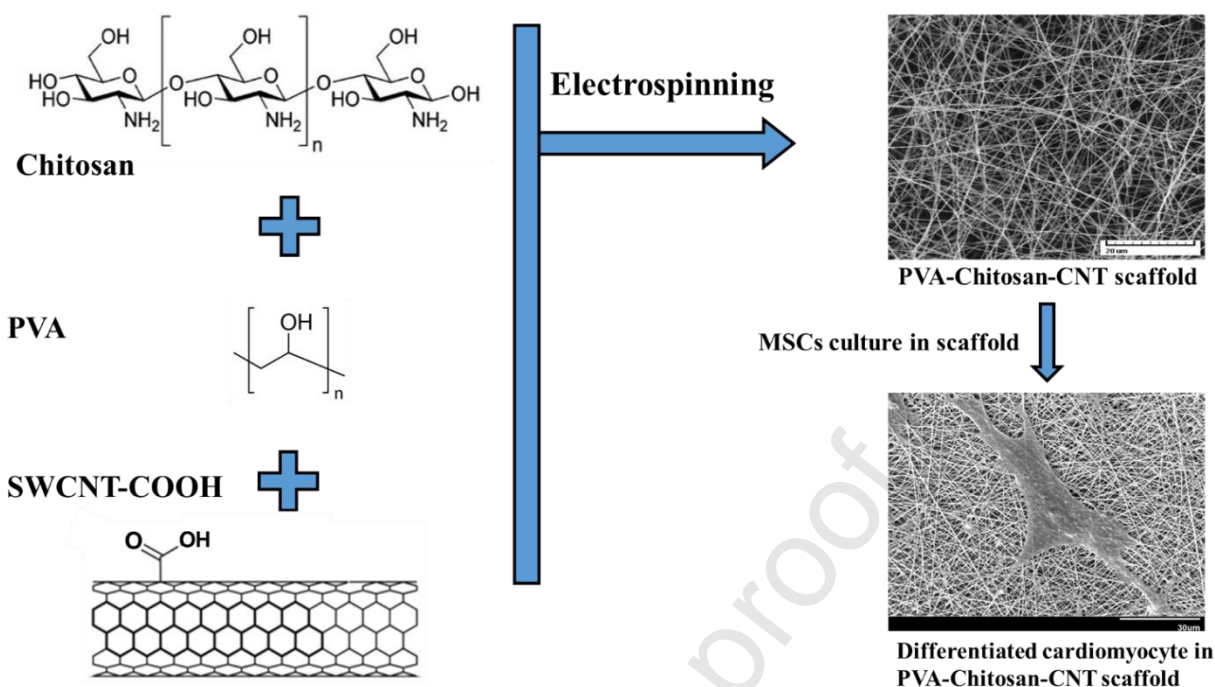
^aCorresponding Author Email: mohamadnejad@ut.ac.ir. Fax: 1439957131, Tehran, Iran, Tel 00989124186330-009821611155775.

^bCorresponding Author Email: b.bakhshandeh@ut.ac.ir.

Highlights

- 1- Nanofiber scaffolds based on polyvinyl alcohol, chitosan and different concentrations of carbon nanotube were produced using electrospinning.
- 2- Nanofiber containing 1% of CNT has optimal properties for cardiac differentiation.
- 3- The qPCR results were indicated that the expression of cardiac marker was increased significantly in comparison to control group.

Graphical Abstract



Abstract

Conductive scaffolds are suitable candidates for cardiovascular tissue engineering (CTE) due to their similarity to the extracellular matrix of native tissue. Here, nanofiber scaffolds based on polyvinyl alcohol (PVA), chitosan (CS), and different concentrations of carbon nanotube (CNT) were produced using electrospinning. Scanning electron microscopy (SEM) image, mechanical test (elastic modulus: 130 ± 3.605 MPa), electrical conductivity (3.4×10^{-6} S/Cm), water uptake, cell adhesion, and cell viability (more than 80%) results of the PVA-CS-CNT1 scaffold revealed that the nanofiber containing 1% of CNT has optimal properties for cardiac differentiation. Afterwards, the differentiation of rat mesenchymal stem cells (MSCs) to cardiomyocytes was performed on the optimal scaffold by electrical stimulation in the presence of 5-azacytidine, TGF- β and ascorbic acid. The real-time qPCR results were indicated that the expression of Nkx2.5, Troponin I, and β -MHC cardiac marker was increased significantly (more than 3 folds) in comparison to control group. Based on the findings of this study, the incorporation of MSCs, conductive scaffolds, and electrical stimulation seem to be a promising approach in CTE.

Keywords: Nanofiber; Chitosan-PVA-CNT nano-complex; Scaffold; Electrical stimulation; Cardiomyocytes differentiation.

Abbreviations: CTE: cardiovascular tissue engineering; PVA: polyvinyl alcohol; Chitosan: CS; carbon nanotube: CNT; MSCs: mesenchymal stem cells; SEM: scanning electron microscopy; RT-qPCR: real time quantitative polymerase chain reaction; DMSO: di-methyl-sulphoxide; MTT: (3-(4,5-dimethylthiazol-2-yl)-2,5-diphenyl tetrazolium bromide; PBS: phosphate buffered saline; TBO: toluidine blue O.

1. Introduction

Cardiovascular disease is the number one cause of death throughout the world. To date, surgical and cell therapies have been widely used for such diseases. However, these approaches are restricted due to the high risk of rejection and unwanted structural changes in body condition [1]. Furthermore, cardiac muscle, as an electroactive tissue, has weak ability to repair itself due to a minimal regeneration potential of cardiomyocytes. Nowadays, there are many approaches including implanting therapeutic cells, biomaterials, and cardiac patches to repair these cardiovascular deficient [2, 3]. On the other hand, cardiovascular tissue engineering (CTE) has been introduced over the past few decades for inducing functional cardiac tissue. Tissue engineering is one of crucial engineering field in which natural, synthetic, or semisynthetic tissue substitutes have been applied for repairing the damaged or diseased living tissues [4]. The scaffolds as conductive and inductive agents are emergent part of tissue engineering that provides a suitable platform for cells as productive agent [4, 5]. On the other hand, use of nanoparticles (NPs) in nanomaterial system offers promising perspectives to development of new approaches in tissue engineering, drug delivery systems, and biosensors [6-9]. Therefore, using the NPs in design and synthesis nanofiber is very affordable in fabrication of scaffolds. Porosity, interconnectivity, biocompatibility, stability, and biodegradability have been considered as excellent properties of NP-based scaffolds which provide three-dimensional (3D) porous platform (pore size less than 10 microns) as real extracellular matrix in cardiovascular tissue engineering (CTE) [8, 10]. Also, high aspect ratio of nanofibers makes them as a great candidate for cell growth, differentiation, and proliferation in tissue engineering.

Using natural-based NPs in fabrication of scaffolds is very suitable method for cardiac cell differentiation applications due to their biocompatibility, excellent mechanical properties, and good conductivity. Chitosan (CS), as a biocompatible biopolymer, is a great biomaterial owing to

non-immunogenic, non-toxic, hydrophilic, hemostatic, and antithrombogenic behavior [11-13]. CS also has utility in fabrication of suitable hydrogel for improving heart function. On the other hand, carbon nanotubes (CNTs) with rolled-graphite sheet and diameters ranging from 0.4 to <100 nm are excellent candidate for scaffolds and due to their specific aspects can provide suitable platform to cell adhesion, morphogenesis, proliferation, and signaling [14, 15]. Furthermore, low material degradation rates, suitable conductivity, and altered mechanical properties are considered as advantage of CNTs. Single-walled carbon nanotubes (SWCNTs) as a single graphite sheet CNTs, demonstrate specific combination of mechanical strength (Young modulus = 0.6-1.25 TPa) and low electrical resistance (resistivity = $1 \mu\Omega\cdot\text{cm}$) that make them as unique nanomaterials for scaffold fabrication and tissue engineering [16]. Moreover, in order to increase the dispersion and stabilization of CNTs in different polar solution, several dispersion techniques such as covalent functionalization with chemical functional groups (such as carboxylation) and protonation have been developed which make it easy to use CNTs in tissue engineering [15, 17]. For example, polyvinyl alcohol (PVA) can improve the solubility of CNTs by formation of hydrogen bonds with CNTs. PVA is also preferentially achievable compound for fabrication of nanofibers that improves the interfacial strength and mechanical performance of scaffolds [18]. On the other hand, biopolymers such as CS, as stabilizing agents, can increase the solubility of CNTs and improve the efficient fabrication of scaffolds with different fabrication methods such as electrospinning, self-assembly, and phase separation techniques. Among these methods, electrospinning due to simplicity, capability to fabricate the nanoscale fibers with great control over fiber dimensions is proposed as a preferable method for nanofiber fabrication [19]. Another most important case in tissue engineering is cell type. Mesenchymal stem cells (MSCs), as multipotent cells with a high degree of flexibility, have demonstrated excellent performance for clinical applications and regenerative biomedicine. MSCs due to great differentiation potential and self-renewing ability can differentiate into many different mature cells such as cardiomyocytes, osteoblasts, chondrocytes, etc. and create different cells with different performance [20, 21].

On the basis of these considerations, the aim of this research is fabrication of PVA-CS-CNT scaffold as natural-based platform for cardiomyocytes differentiation in tissue engineering. To achieve this, different forms of PVA-CS-CNT nanofibers (as scaffolds) were firstly synthesized by electrospinning technique and subsequently, were characterized by means of SEM. Secondly,

different properties of these scaffolds including viscosity, electrical conductivity, values of carboxylic acid functional groups on CNTs, elastic modulus and tensile strength, and amount water uptake were effectively evaluated. Thirdly, in vitro studies including MSCs growth and proliferation, cell viability and gene expression profile of differentiated cardiomyocytes were investigated.

2. Materials and methods

2.1. Materials and apparatus

CS (Mw: 190000-310000 Da (based on viscosity), degree of *N*-deacetylation (75-85%)) and CNT (single-walled >70% (TGA)) were purchased from Sigma-Aldrich, USA. PVA (Mw: 86.09 g/mol; density: 1.19-1.31 g/cm³), glutaraldehyde, hydrochloric acid (HCl), and acetic acid were purchased from Merck, Germany. Di-methyl-sulphoxide (DMSO), toluidine blue O, penicillin, streptomycin, and foetal bovine serum (FBS) were purchased from Sigma-Aldrich. MTT (3-(4,5-dimethylthiazol-2-yl)-2,5-diphenyl tetrazolium bromide) and bovine serum albumin were obtained from Sigma-Aldrich, USA.

SEM (Evo18 ZIESS, Germany), thermal cycler C1000 and real-time thermal cycler (Bio Rad, USA), gel documentation system (Bio Rad, USA), Nanodrop 2000c UV-vis spectrophotometer (Thermo scientific), ultrasonic Homogenizer (Development of Ultrasonic Technology, Iran), ELISA reader (Biotek, USA), and inverted microscope (AE31, China) were used for characterization and evaluation of the performance of the resultant nanomaterial system.

2.2. Scaffold preparation

For this preparation, the CS was firstly dissolved in 2% (v/v) acetic acid to obtain a 3% (w/v) solution. This solution was stirred at 200 rpm for overnight. Then, PVA solution (8% v/v) was prepared with dissolving PVA in double-distilled water at 150 rpm and 50 °C for 2 hours. Afterward, PVA and CS solutions were mixed with each other (with 96:4 w/w ratio) and CS-PVA solution was obtained.

In the second phase, different ratios of CNT NPs (1 wt%, 3 wt%, 5 wt%) were dissolved in 100 µl of ethanol solution. After sonication (20 minutes with a frequency of 70 MHz) of these solutions using ultrasonic homogenizer, mono-disperse solutions of CNT NPs were obtained.

Subsequently, these solutions were separately added to certain amounts of CS-PVA solutions (4 wt% of CS and 96 wt% of PVA) and were sonicated for 30 minutes again to achieve PVA-CS-CNT nano-complexes (PVA-CS-CNT1, PVA-CS-CNT3, and PVA-CS-CNT5).

In the third phase, the solutions were transferred into a 1 ml plastic syringe with a stainless steel needle having the outer diameter of 18 gauges (equivalent to 1.270 mm) which was connected to a high voltage power supply. To electrospin the solutions, the electrospinning equipment was set as follows: voltage 10 kV, feeding rate 0.25 ml per hour, nozzle to mobile collector distance of 11 cm, collector speed of 300 rpm. Eventually, in order to excellent crosslinking the nanofibers, the as-formed nanofibers were treated by glutaraldehyde gas and HCl (with 10:1 ratio) and after incubation at 70 °C for 2 hours, they were washed with glycine [22, 23]. Afterwards, all of the above-mentioned nanofibers were immersed in alcohol (70%) and phosphate buffered saline (PBS) containing 1% of gentamicin for 45 and 10 minutes (for three times), respectively; and were saved in a sterile condition. The scaffold viscometry, porosity, fiber diameter, fiber size, amounts of carboxyl chemical agents, and conductivity were measured.

2.3. Scanning electron microscopy analysis

Scanning electron microscopy (SEM) was used to evaluate the scaffold morphology, porosity, distribution, and infiltration of the cells. To achieve this, nanofibers were washed in PBS. The samples were then sputter-coated with gold and examined by using an SEM at 15 kV (Evo18 ZIESS, Germany). Also, the mean size and dispersity of nanofibers were evaluated with Image J analyzer.

2.4. Measurement of the viscosity of nanofibers

In order to evaluate the formation quality and connectivity of nanofibers, 5 ml (0.3 wt%) of PVA-CS, PVA-CS-CNT1, PVA-CS-CNT3, and PVA-CS-CNT5 nanofibers were prepared and their viscosities were determined by means of the stress-controlled rheometer (Malvern Kinexus Pro). Measurements were done on nanofluids of different nanofibers in a cone and plate configuration with temperature range 40-80 °C (with intervals of 10 °C, n = 3) [24].

2.5. Toluidine blue O test

In order to determine the carboxylic acid group amounts after CNT crosslinking with CS-PVA nanofibers, toluidine blue O (TBO) titration was carried out [25]. As 20 ml of a 0.5 mM TBO solution (pH 10) was firstly prepared. Then, 0.12 mg.ml⁻¹ of prepared nanofibers (PVA-CS-CNT1, PVA-CS-CNT3, and PVA-CS-CNT5) were added to this solution at 30 °C for 4 hours. In the next step, non-complexed TBO on the nanofibers was washed with 30 ml of 0.1 M NaOH for 2 minutes. Subsequently, the complexed TBO was desorbed from the nanofibers with 5 ml of 40 %-v/v acetic acid for 30 minutes. Desorbed TBO was quantified by nanodrop UV-vis spectroscopy at 633 wavelength (n = 3) according to below equation in which “Qt” is amount of TBO absorption per g (mol.g⁻¹) of absorbance in specific time; “C0” and “Ce” are primary and equilibrium concentrations (M) of TBO; “V” is volume (L) of solution; “m” is weight (g) of absorbance:

$$Q_t = (C_0 - C_e) V / m$$

2.6. Electrical conductivity of nanofibers

The electrical conductivity of the nanofibers was measured at room temperature using a UT70A conductivity meter (n = 3) (UT70A: digital multimeter (Lodz, Poland) voltage measuring range: 200mV/2V/20V/200V/1000V; voltage measuring accuracy: ±(0.5% + 1 digit); current measuring range: 20μA/2mA/200mA/10A; current measuring accuracy: ±(1.5% + 1 digit)). The voltage was varied from – 0.5 to 0.5 V, in steps of 0.001 V at 2 seconds intervals, and the current was measured within a Faraday cage to shun electromagnetic field interference. So the volume resistivity (R) was calculated according to the following equation in which “V” is the applied voltage and “I” is the measured current:

$$R = V / I$$

Also, the electrical conductivity (σ) was calculated according to the below equation in which “L” and “A” are the distance between electrodes and area of the electrodes, respectively:

$$\sigma = L / R.A$$

2.7. Mechanical properties of scaffolds

The dynamic aspect measurements of scaffolds such as elastic modulus and tensile strength diagram were performed using a zwick/roel z050 dynamic mechanical analyzer. To achieve these measurements, several scaffolds (3 mm diameter × 4 mm thick discs) were practically

prepared ($n = 3$) and their mechanical characteristics were ascertained. The elastic modulus of different scaffolds was measured in a frequency range of 0.1-5 Hz, at 37 °C and their mechanical properties were compared.

2.8. Water uptake degree of scaffolds

Water uptake study was performed by incubating the PVA-CS, PVA-CS-CNT1, PVA-CS-CNT3, and PVA-CS-CNT5 scaffolds ($n = 3$) in phosphate buffered saline (PBS, pH 7.4) [26]. In order to this evaluation, a known weight of the PVA-CS-CNT1, PVA-CS-CNT3, and PVA-CS-CNT5 scaffolds was immersed in PBS until the swelling equilibrium was reached. Then, the degree of water uptake and swelling (swelling index (SI)) of these samples were calculated according to following equation in which W_d and W_f are denoted the weights of the sample and dried sample, respectively:

$$SI = (W_d - W_f) / W_f$$

2.9. Cell extraction and culture

For this experiment, undifferentiated mesenchymal stem cells (MSCs) were isolated from thighbone marrow of young male rat (20 days). As two ends of bone were separated from the epiphysis area and after removing joint, the marrow sample was washed with Dulbecco's PBS, and cells were recovered after centrifugation at 800g. Subsequently, after transferring nucleated cells onto 20 ml of Dulbecco's modified Eagle's medium (DMEM) solution in a 50-ml conical tube, these cells were centrifuged at 1200g for 25 minutes at 25°C that followed with collecting nucleated cells from the upper layer [27]. Then, these cells were cultured in DMEM (low glucose) containing 10% FBS, 100 µg/ml streptomycin, and 100 IU/ml penicillin. Afterwards, MSCs were cultured in 75 ml flasks using 12 ml of culture medium [27-30]. The grown cell were passaged for several times to obtain homogeneous MSCs and eventually, removed from the bottom of flask using 0.2% of trypsin-EDTA to add to the cell culture plates. On the other hand, a number of 4×10^5 MSCs were seeded in scaffolds (5 mm diameter \times 2 mm thick discs) in medium-containing six-well plates. After 60 minutes, 5 ml of culture medium (20% FBS) was added to each well [27, 29].

The evaluation of MSCs differentiation to cardiomyocytes was carried out in three groups of MSCs: (1) differentiation of MSCs without scaffold, including control group, differentiation with

differentiation medium after 10 days, and differentiation with differentiation medium after 20 days; (2) differentiation of MSCs in scaffold, including differentiation in scaffold without differentiation medium and differentiation in scaffold with differentiation medium after 20 days; (3) differentiation of MSCs in scaffold with differentiation medium and external electrical stimulation after 10 and 20 days.

Differential medium content was including 20 μ l of 5-azacytidine, 1.5 μ l of ascorbic acid, and 1 ng.ml⁻¹ TGF- β which was added to MSCs plates twice a week to help MSCs differentiation to cardiomyocytes. Electrical voltage for stimulation of MSCs was 5 mV.cm⁻¹ in a frequency of 1 Hz for 5 days at 37 °C.

2.10. Cell viability assay

In order to evaluate the cytotoxicity of the scaffolds, MSCs were cultured on the PVA-CS-CNT1, PVA-CS-CNT3, and PVA-CS-CNT5 nano-complexes scaffolds. This evaluation carried out using MTT assay for 1, 3, 7, and 14 days intervals. Therefore, 1 \times 10⁴ cells were added to the cell culture plates (96 wells) containing the nano-complexes scaffolds (5 mg.ml⁻¹ of every scaffold) and MSCs were cultured in DMEM containing 10% FBS. At the end of each time period, the supernatant was removed and washed with PBS and an amount of 100 μ l of culture medium (DMEM) and containing 10 μ l of sterile filtered MTT solution was added to each well. Then, after 4 hours of incubation of cells in dark condition at 37 °C, RH of 98%, and 5% CO₂, the suspension liquid was removed and the cells were re-suspended in 200 μ l of DMSO. In the following, the optical density (OD) of these DMSO solutions was read at wavelength of 570 nm (with ELISA reader apparatus: Biotek, USA) to determine the number of viable cells [27, 31]. Eventually, the cell viability values were compared with groups of cells that were cultured in DMEM medium without scaffolds treatment as a control group.

2.11. Gene expression

The expression profiles of specific-cardiac markers (Nkx2.5, Troponin I, and β -MHC) were evaluated by real-time quantitative PCR (RT-qPCR) [32, 33]. As cellular RNA of cardiac cells after 10 and 20 days was extracted using RNA extraction kit according to the manufacturer's instructions (Thermo Scientific, USA). In order to remove the possible contamination of DNA, the extracted RNA samples of specific-cardiac cells were treated with the enzyme DNase 1.

Then, quantity and purity of RNA were determined using a NanoDrop spectrophotometer. In the following, 4 μ l of RNA was taken up and were synthesized using the cDNA synthesis kit (Thermo Scientific, USA), random hexamer primers, and reverse transcriptase enzyme. Afterwards, RT-qPCR analysis was carried out. As RT-qPCR was performed with a 14 μ l reaction mixture containing 1 μ l of cDNA, 7 μ l of low rox Master mix real time, and 0.5 μ l of forward primers (Troponin-I gene: 5'CCATGATGCAGGCACTACTGGG3' ; Nkx2.5 gene: 5'ACCCTCGGGCGGATAAGAA3' ; β -MHC gene: 5'ATCAAGGGAAAGCAGGAAGC3') and reverse primers (Troponin-I gene: 5'GGTTTTCTTCTCAATGTCCTCCTTC3' ; Nkx2.5 gene: 5'GACAGGTACCGCTGTTGCTTGA3' ; β -MHC gene: 5'CCTTGTCTACAGGTGCATCA3'), and 7 μ l of DDW. Subsequently, PCR temperature was applied using RT-qPCR apparatus: heating at 95 °C for 15 min, 45 cycles at 95 °C for 20 seconds, annealing at 60 °C for 30 seconds, and elongation at 72 °C for 20 seconds. Ultimately, cardiac genes expression were normalized to glyceraldehyde-3-phosphate-dehydrogenase (GAPDH), and results were calculated as fold change relative to the control (PVA-CS-CNT1-cell and CS-PVA-cell, n = 5 per group and time point).

2.12. Statistical analysis

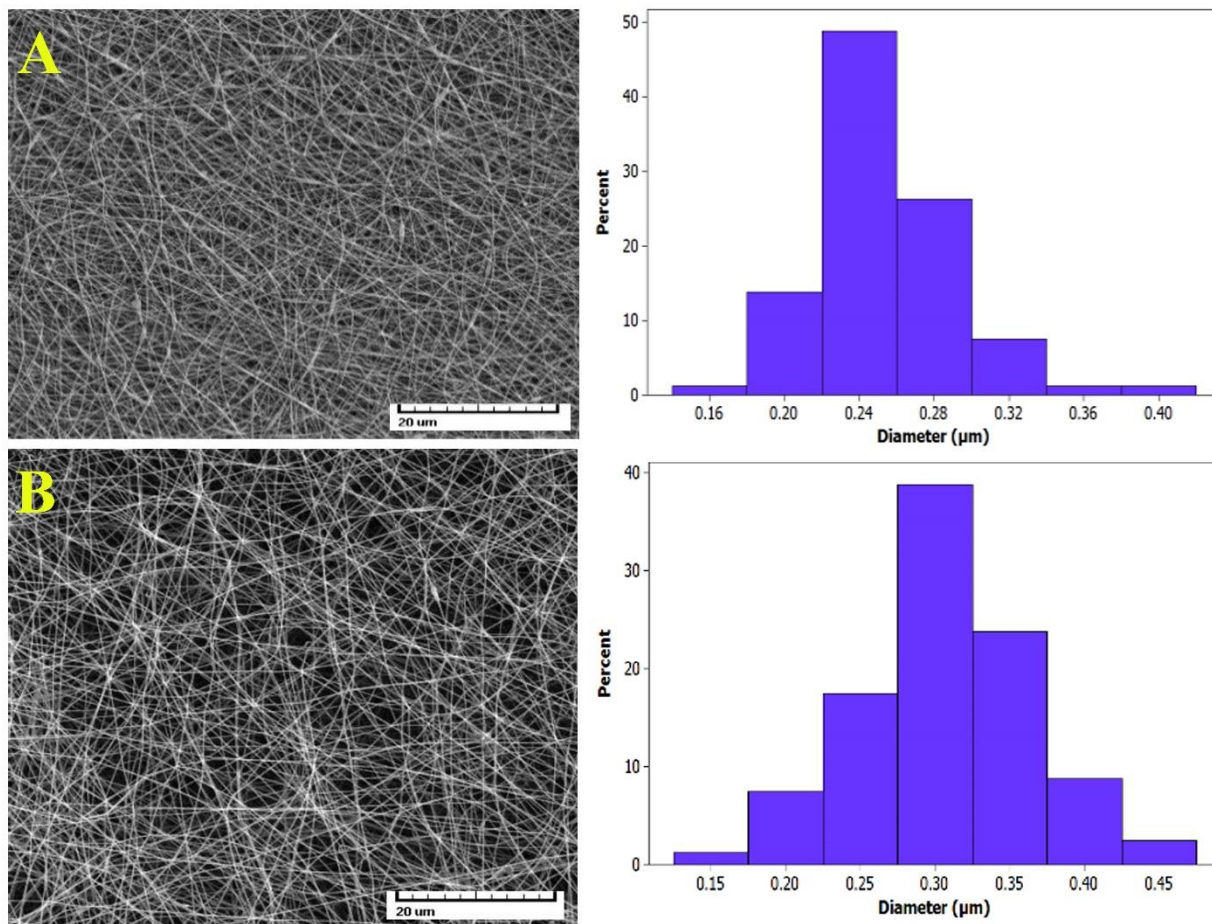
In this study, to compare between the various groups, the statistical differences were evaluated using the one-way ANOVA and Tukey's HSD with considered significance at $p < 0.05$. Results are expressed as mean \pm SD, with n = 3 per group and time point.

3. Results and discussion

3.1. Scanning electron microscopy analysis

The porosity and pore interconnectivity of scaffolds (CS-PVA, PVA-CS-CNT1, PVA-CS-CNT3, and PVA-CS-CNT5 nano-complexes scaffolds) were determined by SEM analysis (Figure 1). As shown in this figure, the complete porous microstructure with continuous and interconnected porosity are significantly revealed. As the diameter of the nanofibers were 255 ± 3.5 nm, 292 ± 5.5 nm, 295 ± 4.2 nm, and 307 ± 5.9 nm for CS-PVA, PVA-CS-CNT1, PVA-CS-CNT3, and PVA-CS-CNT5 scaffolds, respectively (Figure 1). It is clearly demonstrated that increasing the percentage of CNTs in different formulations led to rising in the diameter of nanofibers which is due to the high viscosity of nanofibers after using the high percentage of

CNT. On the other hand, the nano-complexes scaffolds have a fully fibrous and porous structure with interconnected pores which can provide a suitable platform and extracellular matrix for diffusion of essential nutrients and oxygen for cell survivability [34].



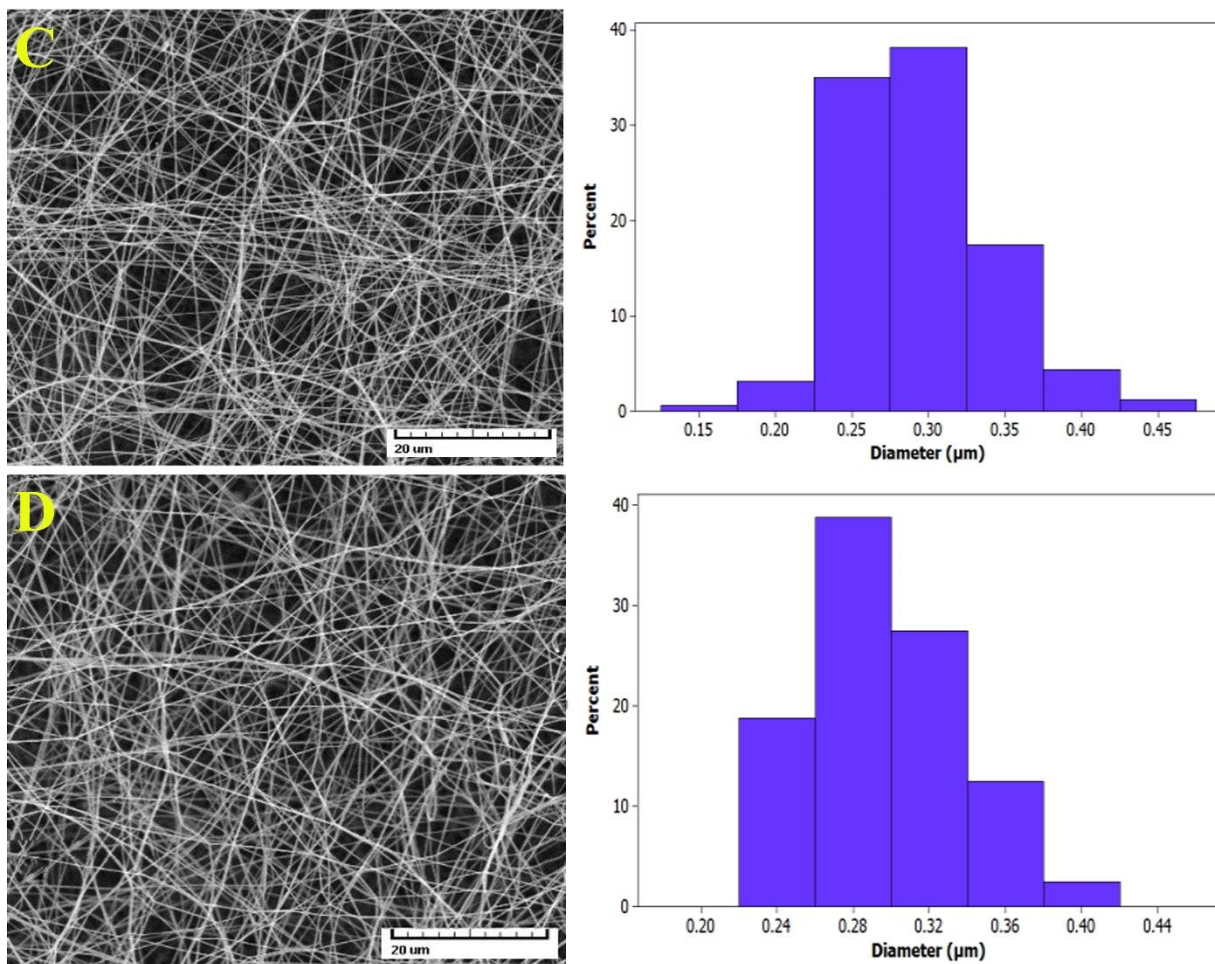


Figure 1. SEM micrograph of CS-PVA (A), PVA-CS-CNT1 (B), PVA-CS-CNT3 (C), and PVA-CS-CNT5 (D) nanofibers (Scale bar is 20 μm). The porosity, pore interconnectivity of scaffolds and mean diameter of nanofibers are clearly shown. By increasing the percentage of CNT in different nanofibers, the diameters increase.

3.2. Viscosity of nanofibers

Viscosity is one of the main elements in continuous formation of nanofibers which can help to integrate and non-granular formation of nanofibers. Actually, viscosity of the spinning solution is very important for being able to produce a continuous flowing stream of polymer from the needle to the collector [35]. The viscosity of the CS-PVA, PVA-CS-CNT1, PVA-CS-CNT3, and PVA-CS-CNT5 solutions was measured using the viscometer (Table 1). As CS-PVA was shown lower and PVA-CS-CNT5 was demonstrated higher viscosity. As a matter of fact, CNT leads to increasing the nanofiber viscosity due to its carboxylic (COOH) functional group and

subsequently, increases the formation of hydrogen bonds between the CNT and CS and PVA. These bonds lead to high viscosity in PVA-CS-CNT5 nanofiber solution. In fact, adding the CNT to the polymer solutions, leading to a slight increase in the viscosity [24, 35]. Also, average porosities of nanofibers fabricated with electrospinning method were 70% to 80%.

Table 1. Viscosity values of different nano-complexes.

Nano-complexes	PVA (v %)	CS (v %)	CNT (v %)	Viscosity (Mpa.s)
PVA-CS	72	28	0	178.643 ± 1.088
PVA-CS-CNT1	66	25	8	188.233 ± 1.961
PVA-CS-CNT3	57	21	21	210.836 ± 0.804
PVA-CS-CNT5	50	18	27	238.083 ± 2.478

3.3. Toluidine blue O test

In order to evaluate the amount of CNT carboxylic functional group of synthetic nanofibers after CS crosslinking with citric acid, this test was performed. In this test, the interaction between carboxylic acid, acetic acid, and toluidine blue molecules lead to the creation of specific color which is detectable by means of the NanoDrop spectrophotometer. High absorption intensity indicates high amounts of the carboxylic acid functional group [25]. The carboxylic acid functional groups improve the dispersity of polymeric solution which subsequently it leads to the monotonous formation of nanofibers. Also, high values of carboxylic acid groups lead to increasing mechanical properties that are most important for scaffold [15, 25]. The results of this test showed that PVA-CS-CNT5 scaffolds have the high amount ($698 \pm 25.82 \text{ mol.gr}^{-1}$) of the carboxylic acid functional group (figure 2A). Also, PVA-CS-CNT1 ($421 \pm 19.02 \text{ mol.gr}^{-1}$) and PVA-CS-CNT3 ($548 \pm 32.83 \text{ mol.gr}^{-1}$) scaffolds have high amounts of carboxylic acid groups (Figure 2A).

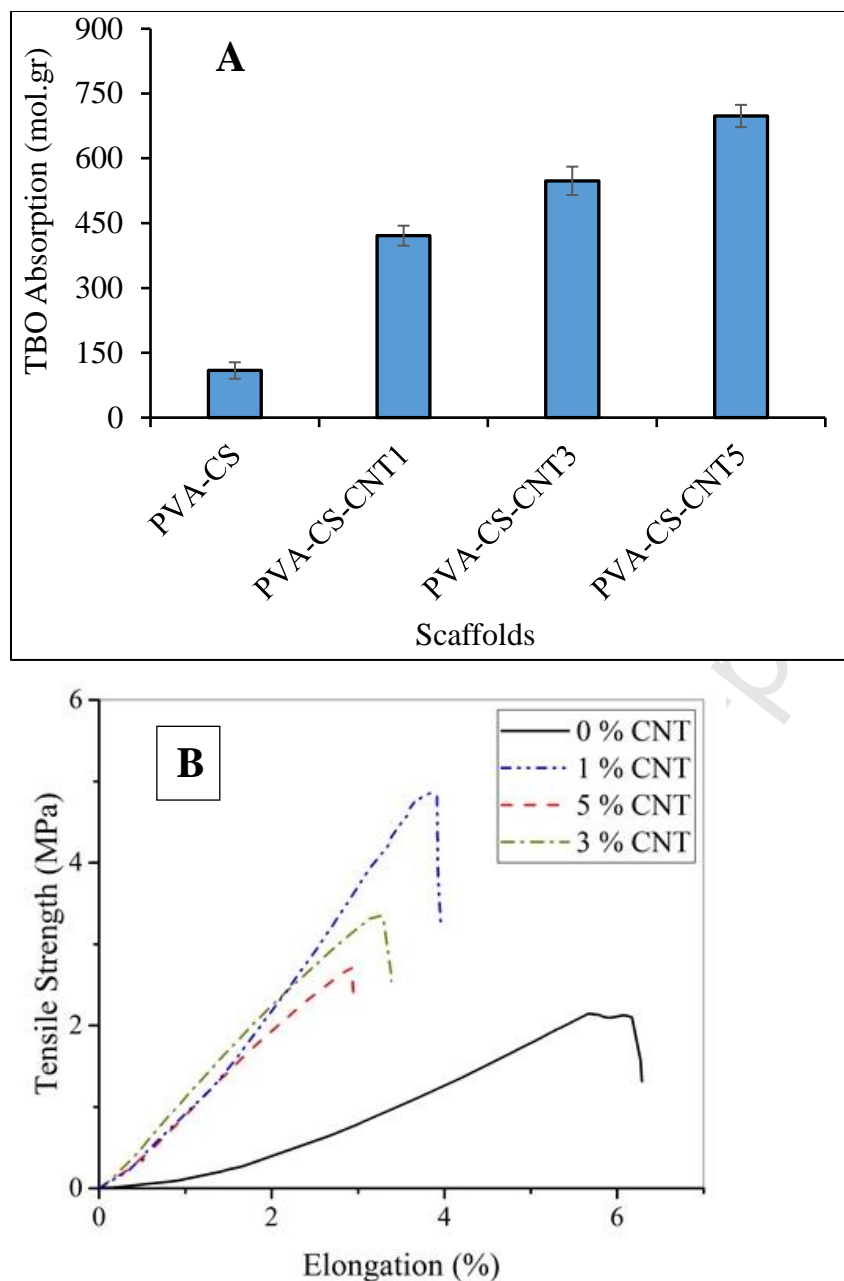


Figure 2. Absorption values of toluidine blue for different scaffolds (A). In terms of their carboxylic acid values, samples can be arranged as following order: PVA-CS-CNT5 > PVA-CS-CNT3 > PVA-CS-CNT1 > PVA-CS. The tensile strength of scaffolds (B).

3.4. Electrical conductivity of nanofibers

The electrical conductivity of PVA-CS-CNT1, PVA-CS-CNT3, and PVA-CS-CNT5 scaffolds, measured in a dry state at room temperature. Based on fundamental literature, there are different parameters affecting the conductivity of the CNT containing nanofibers including the

conductive property of CNT, CNT size and concentration, and CNT dispersion in solution [36]. The electrical conductivity of PVA-CS-CNT1, PVA-CS-CNT3, and PVA-CS-CNT5 scaffolds was determined 3.4×10^{-6} S/Cm, 4.1×10^{-5} S/Cm, and 1.63×10^{-6} S/Cm, respectively. As it was revealed, the conductivity of PVA-CS-CNT5 was considerably decreased that probably was due to the high concentration of CNT. In this concentration, the possible distance between the CNTs decreases and ultimately increases the possible contact between the CNTs that makes interference in conductivity of scaffold network. These conductivities of scaffolds are related to the unpaired electrons of CNT. Actually, Sp^2 hybridization occurs among carbon atoms and an unpaired electron of each carbon atom is on π orbit that is perpendicular to the layers [36]. On the other hand, the native myocardium possesses a conductivity with the range from 1.6×10^{-5} S/cm (longitudinally) to 5×10^{-5} S/cm (transversally) that are close to the conductivity of the scaffolds in this work ($4.3\text{--}15.7 \times 10^{-4}$ S/cm). Furthermore, Zhao et al. [37] synthesized a series of gelatin-polyaniline conductive hydrogels (as scaffold for MSCs) with the conductivity from 1.3×10^{-3} to 1.6×10^{-3} S/cm, and their results demonstrated that this conductivity could increase the MCSs proliferation. Therefore, the electrical conductivity of our nanofibers might be suitable for heart tissue engineering and cell proliferation.

3.5. Mechanical properties of scaffolds

Table 2 and figure 2B presents the changes in elastic modulus and tensile strength diagram of different scaffolds. By increasing the weight percent of CNT from 1 wt% to 5 wt%, elastic modulus and tensile strength of scaffolds were considerably decreased. As the elastic modulus and tensile strength of PVA-CS were increased when the low percentage of CNT (1 wt%) was used in the content of nanofiber; however, increasing the weight percent of CNT from 1 wt% to 3 wt% and 5 wt% leading to low elastic modulus and tensile strength in PVA-CS-CNT3 and PVA-CS-CNT5 scaffolds. These two scaffolds indicate poor mechanical properties due to the high content of their heterogeneous nature [38]. On the other hand, agglomeration of nanoparticles in high concentration and lack of monodispersity in the solution of 3 wt% and 5 wt% CNTs interface in formation of the polymeric matrix that eventually, decrease the mechanical properties of PVA-CS-CNT3 and PVA-CS-CNT5 scaffolds [38, 39]. Therefore, these results revealed that the CNT (especially in low weight percent) can significantly reinforce

scaffolds mechanical tensile strength, elastic modulus, and stability as reported by Zhao et al. research previously [40].

Table 2. The elastic modulus and tensile strength of scaffolds

Scaffolds	Tensile strength (MPa)	Elastic modulus (MPa)
PVA-CS	2.1 ± 1.088	30 ± 3.01
PVA-CS-CNT1	4.9 ± 1.961	130 ± 3.605
PVA-CS-CNT3	3.4 ± 0.804	121 ± 2.516
PVA-CS-CNT5	2.7 ± 2.478	101 ± 1.527

3.6. Water uptake degree of scaffolds

The CS, PVA, and carboxylic acid-modified CNT are naturally hydrophilic materials. Therefore, these nanomaterials have suitable solubility in water with pH, 7 without crosslinking. However, after crosslinking they become complete water-insoluble materials which makes them as excellent candidate for being suitable platform in tissue engineering. Figure 3 shows the water uptake of PVA-CS, PVA-CS-CNT1, PVA-CS-CNT3, and PVA-CS-CNT5 scaffolds in PBS at pH 7.4 after 12, 24, and 36 hours. The lower water uptake was obtained for PVA-CS-CNT5 scaffolds. Generally, the water uptake behavior of PVA-CS-CNT1 ($20.21 \pm 2.2 \text{ gr.gr}^{-1}$ after 36 hours) and PVA-CS-CNT3 ($18.27 \pm 1.9 \text{ gr.gr}^{-1}$ after 36 hours) scaffolds was increased in comparison to PVA-CS and PVA-CS-CNT5 scaffolds. These results indicate that CNTs lead to more monodispersity of PVA-CS-CNT1 scaffolds by increasing its solubility and facilitating hydrogen bond formation between CNT and water molecules. Hydrogen bonds improve water absorption. Suitable dispersity of CNT in PVA-CS-CNT1 scaffold resulting in formation of monotonous scaffolds with desirable molecular distance between PVA, CS and CNT that subsequently, facilitates infiltration of H_2O molecules in PVA-CS-CNT1 scaffold [22, 23]. Moreover, by increasing the CNT content in scaffolds (PVA-CS-CNT3 and PVA-CS-CNT5 scaffolds), crosslinking density of scaffolds increase that leads to decreasing the water uptake ability of scaffolds. These results are in line with Zhao et al. work [40].

This desirable water absorption ability of PVA-CS-CNT1 scaffold indicates that this scaffold can provide an excellent platform for cell growth and proliferation because nutrients can easily flow and uptake from its fibrous structure in the body and reach to cells when they need to nutrients. On the other hand, suitable water uptake facilitates slow degradation of this scaffold in wet body condition that is necessary in tissue engineering. Furthermore, CNT enhances chemical stability and crosslinking makes the PVA-CS-CNT1 scaffolds as a suitable platform for tissue

engineering [22, 41]. PVA-CS-CNT3 scaffold also followed the same way. However, PVA-CS-CNT5 scaffold shows less water uptake in comparison to PVA-CS scaffold that is due to heterogenous dispersity of CNT in PVA-CS-CNT5 scaffold and much more amounts of carboxylic acid modified CNTs. On the other hand, by formation much more hydrogen bonds between CS and CNTs, PVA preserves from the formation of hydrogen bond with H₂O molecules.

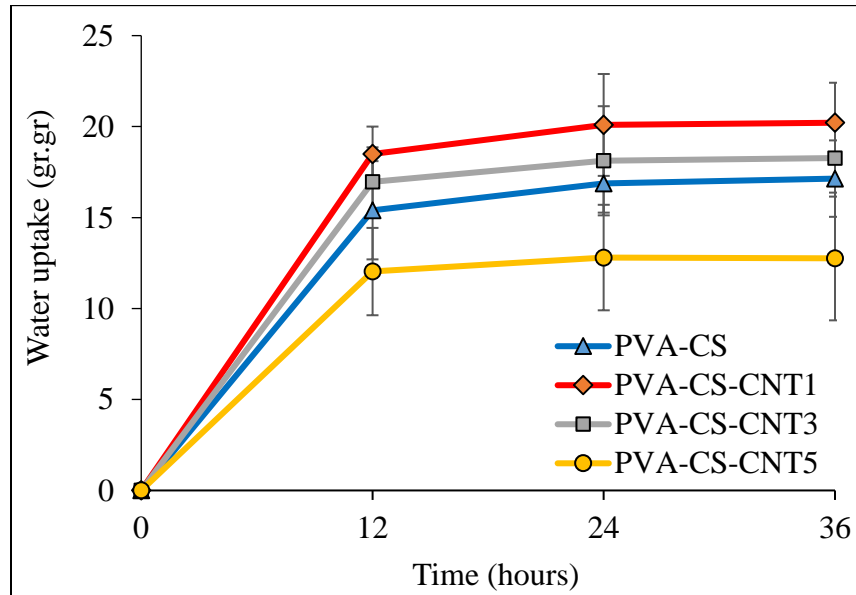


Figure 3. Water uptake degree of PVA-CS, PVA-CS-CNT1, PVA-CS-CNT3, and PVA-CS-CNT5 scaffolds in PBS at pH 7.4 after 12, 24, and 36 hours.

3.7. Cell viability assay

In order to evaluate the viability of cells on the PVA-CS, PVA-CS-CNT1, PVA-CS-CNT3, and PVA-CS-CNT5 scaffolds, MTT assay was applied to investigate the cytotoxicity of these scaffolds against MSC cell (Figure 4). This assay was carried out at 1, 3, 7, and 14 days after treatment with different scaffolds (5 $\mu\text{g}.\text{ml}^{-1}$ per every scaffold). As can be seen in figure 4, PVA-CS-CNT3 and PVA-CS-CNT5 scaffolds demonstrating more cytotoxic effects than other scaffolds (PVA-CS, PVA-CS-CNT1) on MSCs. As high concentrations of CNT in PVA-CS-CNT3 and PVA-CS-CNT5 scaffolds led to $59.93 \pm 5.98 \%$ and $56.38 \pm 4.98 \%$ of cell viability after one day post-treatment time, respectively; while it was $91.72 \pm 4.23 \%$ and $90.32 \pm 6.21 \%$ of cell viability for PVA-CS and PVA-CS-CNT1 at the same time which is due to their biocompatibility [42, 43]. By compare the cytotoxic effects of these scaffolds on MSC cell, it

was concluded that PVA-CS and PVA-CS-CNT1 have not remarkable toxic effects on MSC cell. One of the possible explanation to high cytotoxic effects of PVA-CS-CNT3 and PVA-CS-CNT5 scaffolds is this fact that carboxyl group of CNT as a hydrophilic agent can help to solubility of these scaffolds and subsequently, increases their internalization into MSCs that leads to cell death [43]. On the other hand, CNT absorbs the serum nutrition such as proteins that promotes cell death. Also, high weight percent of CNT in PVA-CS-CNT3 and PVA-CS-CNT5 results in agglomeration of these scaffolds that induces their phagocytosis and subsequently, starts inflammatory responses and cell necrosis in implanted body organ [43, 44]. Furthermore, *in vivo* and *in vitro* studies on CNT cytotoxicity have demonstrated that exposure of cells to high concentration of CNT and its derivatives, promotes oxidative stress and the generation of reactive oxygen species [44]. On the other hand, the possible reason for increasing cell viability in day 3 can be self-adaptation and self-renewal processes in MSCs in which MSCs adapted themselves with new condition [45].

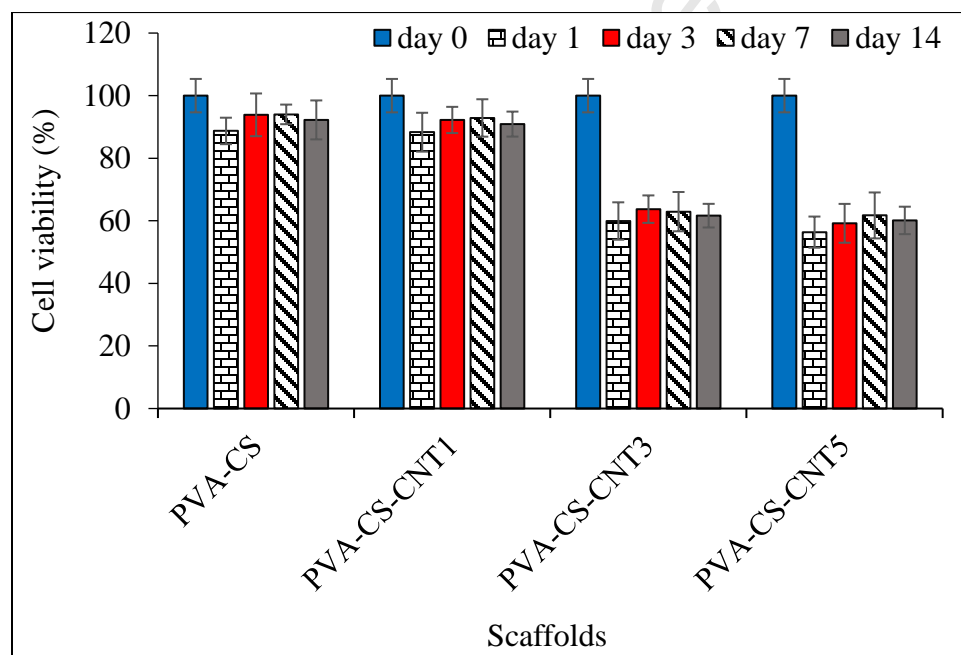


Figure 4. Cell viability of MSC after treatment with different scaffolds (PVA-CS, PVA-CS-CNT1, PVA-CS-CNT3, and PVA-CS-CNT5) at 1, 3, 7 and 14 days post-treatment time.

3.8. Cell growth and attachment to scaffold

Figure 5 shows the SEM micrographs of differentiated MSCs in PVA-CS, PVA-CS-CNT1, PVA-CS-CNT3, and PVA-CS-CNT5 scaffolds after 14 days of exposure to electrical stimulation

(5 mV.cm⁻¹ in a frequency of 1 Hz) differentiation medium (containing 5-azacytidine, TGF- β , and ascorbic acid). The nanostructure and interconnected porosity of scaffolds serve as an excellent medium for cell growth and attachment to stimulate and reorganize the cells [32]. Furthermore, these specific network structures facilitate the nutrient transport and metabolism of cells. Among these scaffolds, PVA-CS and PVA-CS-CNT1 indicate better performance in creating a suitable natural extracellular matrix for MSCs. Moreover, morphological observation was indicated homogeneous dispersion of MSCs throughout PVA-CS and PVA-CS-CNT1 scaffolds, while it was not homogeneous in PVA-CS-CNT3 and PVA-CS-CNT5 scaffolds. On the other hand, MSCs lose the mesenchymal stem cell structure and show crumple cytoplasm form on PVA-CS-CNT3 and PVA-CS-CNT5 scaffolds which demonstrate that these scaffolds are not suitable for cell differentiation. Many research have indicated that electrical stimulation and conductivity contribute to great proliferation and differentiation of electrical signal sensitive cells like cardiomyocytes and other tissues cells. Among conductive materials, polymeric nanoparticles such as CNT and polyaniline have shown excellent application in tissue engineering. In a research by Zhao et al. [37] with the increase of polyaniline content of hydrogel as scaffolds, the number of MSC dead cells were decreased and they exhibited a higher cell proliferation while high concentration of CNT was prevented from cell proliferation in our work. On the other hand, CS as biocompatible material was induced cell proliferation and differentiation in both works that shows excellent biocompatibility of CS as scaffold in tissue engineering.

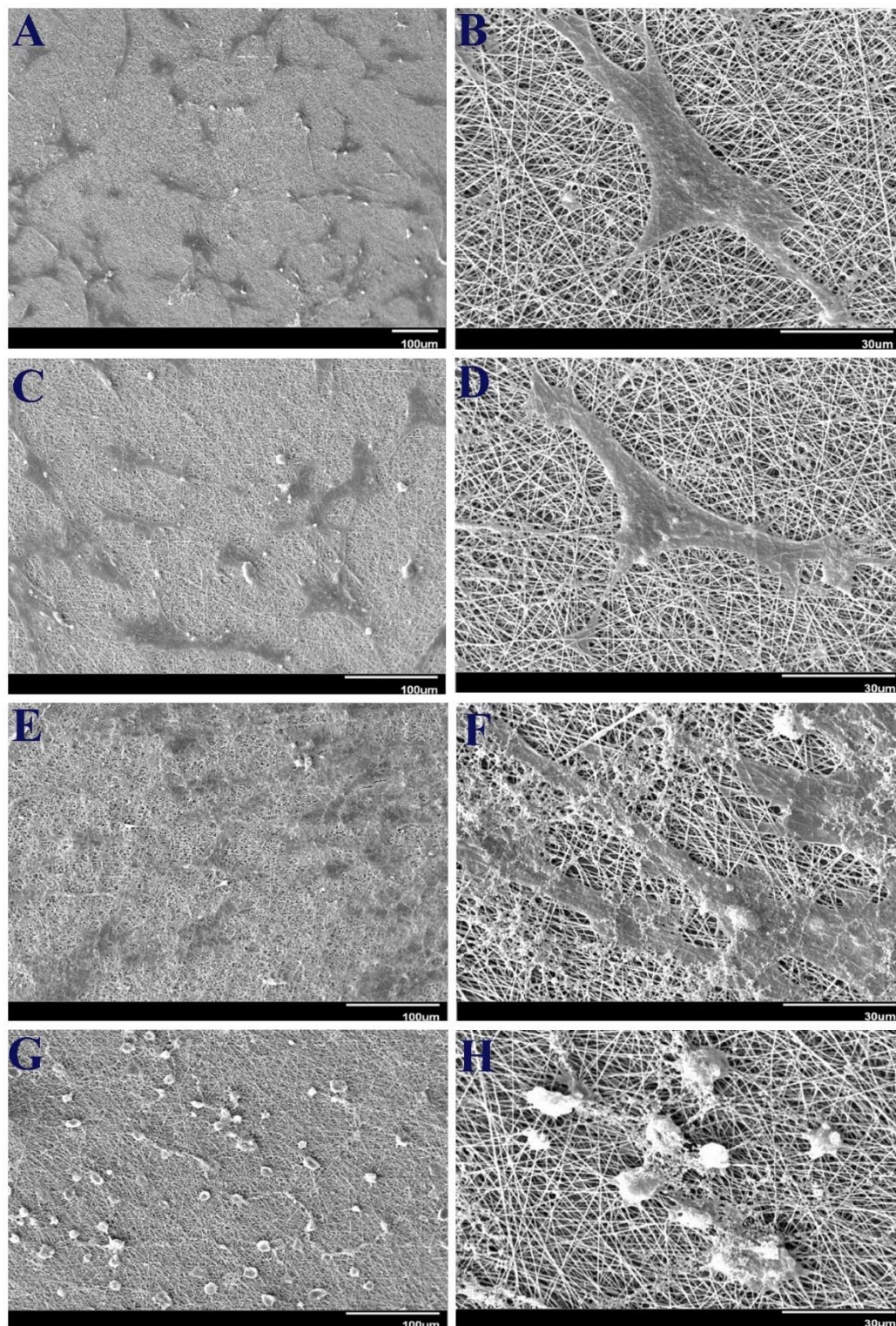


Figure 5. SEM micrographs of MSCs after differentiation to cardiomyocytes in PVA-CS (A, B), PVA-CS-CNT1 (C, D), PVA-CS-CNT3 (E, F) and PVA-CS-CNT5 (G, H) scaffolds after 14 days exposure to electrical stimulation and the differentiation medium. Scale bars are 100 μm for

A, C, E, and G; and 30 μm for B, D, F, and H. Scale bars are 100 μm (for A, C, E, G) and 30 μm (for B, D, F, H).

3.9. Gene expression

Cardiac marker (Nkx2.5, Troponin I, and β -MHC) gene expression profiles were analyzed for cardiomyocytes cultured PVA-CS-CNT1 scaffold. PVA-CS-CNT1 scaffold due to less cytotoxic effect and excellent performance in creating a suitable natural extracellular matrix for MSCs was selected as a suitable platform for cell culture. Therefore, gene expression profiles were evaluated for differentiated cells in this scaffold. Figure 6 displays the results of cardiac gene expression values in different condition and times. As mentioned previously, evaluation of MSCs differentiation to cardiomyocytes was performed in three groups of MSCs: (1) differentiation of MSCs without scaffold, including control group, differentiation with differential medium after 10 days, and differentiation with differential medium after 20 days; (2) differentiation of MSCs in scaffold, including differentiation in scaffold without differential medium and differentiation in scaffold with differential medium after 20 days; (3) differentiation of MSCs in scaffold with differential medium and external electrical stimulation after 10 and 20 days. From the results, the relative amounts of expression of Nkx2.5, Troponin I, and β -MHC increased significantly after exposing differential medium and external electrical stimulation in comparison with the control group (Figure 6). Moreover, the results reveal that differentiation of group 3 MSCs (differential medium and external electrical stimulation after 20 days) is more than 2 folds in comparison to differentiation of MSCs in scaffold with the differential medium after 20 days; and is also more than 4 folds of differentiation of MSCs with the differential medium after 10 days. Also, by compare the gene expression after in culture medium and in scaffold with differential medium and external electrical stimulation after 10 and 20 days, it was concluded that differential medium and external electrical stimulation have the main role in differentiation of cardiomyocytes in PVA-CS-CNT1 scaffold [46]. These results were also compared with Martins et al. work [22]. As the highest gene expression (about 2.6 folds) was observed for cardiac Troponin I that is important for contractile function in muscle tissue while its expression value was about 3.1 folds in our research at the specific period time after culture on scaffold. Thus, PVA-CS-CNT1 scaffold is great candidate for electrically conductive cardiac tissue engineering that stimulates the upregulation of genes associated with the process of cardiomyocytes

differentiation and ultimately, induces the growth of cells [33, 47]. On the other hand, results of RT qPCR approve that the presence of CNT in CS scaffolds facilitated the cardiogenic phenotype and expression of cardiac markers after 10 and 20 days, with external electrical stimulation. Actually, the increased conductivity at the level of PVA-CS-CNT1nanofiber significantly played a crucial role in enhancing gene expression through gradients in voltage and currents around the cells.

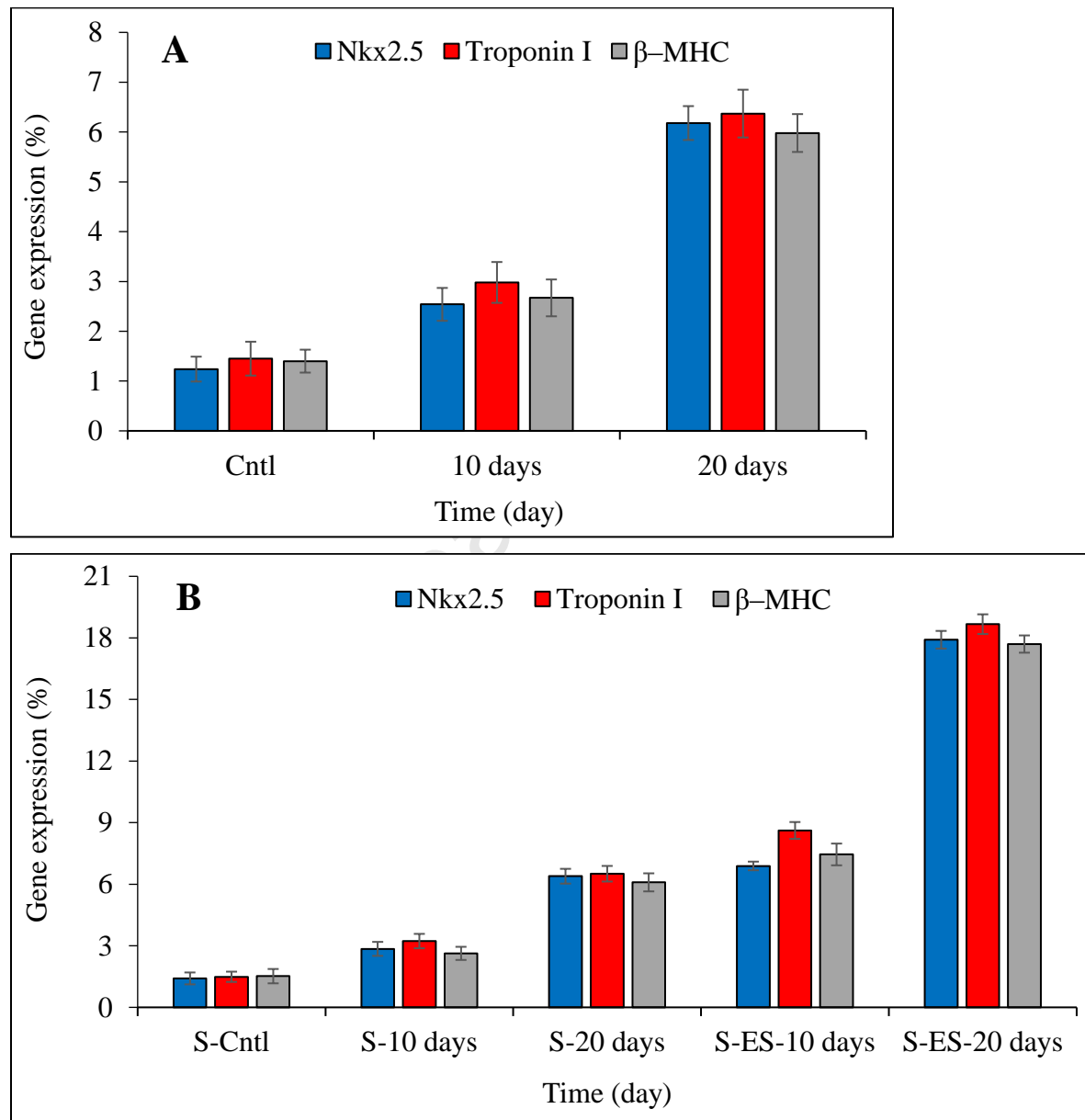


Figure 6. Relative gene expression of Nkx2.5, Troponin I, and β-MHC cardiac marker at days 10 and 20 of cardiomyocytes differentiation of mesenchymal stem cells in PVA-CS-CNT1 scaffold.

Values of gene expression in culture medium without scaffolds (A) and with scaffolds (B). Cntl: control group; S-Cntl: control group in scaffold; S-10 days: cardiomyocytes differentiation of MSCs with differential medium after 10 days; S-20 days: cardiomyocytes differentiation of MSCs with differential medium after 20 days; S-ES-10 days: cardiomyocytes differentiation of MSCs with differential medium and external electrical stimulation after 10 days; S-ES-20 days: cardiomyocytes differentiation of MSCs with differential medium and external electrical stimulation after 20 days.

4. Conclusion

In this research work, electrically conductive PVA-CS-CNT1, PVA-CS-CNT3, and PVA-CS-CNT5 nanofibers were fabricated using the electrospinning method. Mean diameter of the nanofibers were determined 255 ± 3.5 nm, 292 ± 5.5 nm, 295 ± 4.2 nm, and 307 ± 5.9 nm for CS-PVA, PVA-CS-CNT1, PVA-CS-CNT3, and PVA-CS-CNT5 scaffolds, respectively. These scaffolds provide three-dimensional platform for cell proliferation and growth such as extracellular matrix in body tissues. The results were indicated that CNTs significantly increases the conductivity, chemical stability, crosslinking properties, elastic modulus, and tensile strength of scaffolds and enhances the adherence of MSCs to scaffolds. Also, the growth and viability of cultured MSCs were evaluated with MTT assay in fabricated scaffolds and PVA-CS-CNT1 scaffold was selected as non-toxic and suitable platform for cell growth. Gene expression profiling demonstrated upregulation of Nkx2.5, Troponin I, and β -MHC cardiac marker at days 10 and 20 of cardiomyocytes differentiation in PVA-CS-CNT1 scaffold. Ultimately, the incorporation of MSCs, conductive scaffolds, and electrical stimulation seem to be a promising approach in cardiovascular tissue engineering.

References

- [1] B.Z. Tian, J. Liu, T. Dvir, L.H. Jin, J.H. Tsui, Q. Qing, Z.G. Suo, et al., Macroporous nanowire nanoelectronic scaffolds for synthetic tissues. *Nat. Mater.* 11 (2012) 986-994.
- [2] M.C. Yang, S.S. Wang, N.K. Chou, N.H. Chi, Y.Y. Huang, Y.L. Chang, M.J. Shieh, et al., The cardiomyogenic differentiation of rat mesenchymal stem cells on silk fibroinpolysaccharide cardiac patches in vitro. *Biomaterials* 30 (2009) 3757-3765.

- [3] C. Patra, S. Talukdar, T. Novoyatleva, S.R. Velagala, C. Muhlfield, B. Kundu, S.C. Kundu, et al., Silk protein fibroin from *Antheraea mylitta* for cardiac tissue engineering. *Biomaterials* 33 (2012) 2673-2680.
- [4] N. Tandon, A. Marsano, R. Maidhof, L. Wan, H. Park, G. Vunjak-Novakovic, Optimization of electrical stimulation parameters for cardiac tissue engineering. *J. Tissue Eng. Regener. Med.* 5 (2011) 115-125.
- [5] N.K. Satija, G.U. Gurudutta, S. Sharma, F. Afrin, P. Gupta, Y.K. Verma, Mesenchymal stem cells: molecular targets for tissue engineering. *Stem. Cells Dev.* 16 (2007) 7-23.
- [6] A. Narmani, M. Kamali, B. Amini, H. Kooshki, A. Amini, L. Hassani, Highly sensitive and accurate detection of *Vibrio cholera* O1 OmpW gene by fluorescence DNA biosensor based on gold and magnetic nanoparticles. *Process Biochemistry* 65 (2018) 46-54.
- [7] A. Amini, M. Kamali, B. Amini, A. Najafi, A. Narmani, L. Hasani, et al., Bio-barcode technology for detection of *Staphylococcus aureus* protein A based on gold and iron nanoparticles. *Int. J. Biol. Macromol.* 124 (2019) 1256-1263.
- [8] D. Cheng, R. Xie, T. Tang, X. Jia, Q. Cai, X. Yang, Regulating micro-structure and biomineralization of electrospun PVP-based hybridized carbon nanofibers containing bioglass nanoparticles via aging time. *RSC Advances* 6 (2016) 3870-3881.
- [9] A. Narmani, B. Farhood, H. Haghi-Aminjan, T. Mortezaazadeh, A. Aliasgharzadeh, M. Mohseni, et al., Gadolinium nanoparticles as diagnostic and therapeutic agents: Their delivery systems in magnetic resonance imaging and neutron capture therapy. *J. Drug Deliv. Sci. Technol.* 44 (2018) 457-466.

- [10] Y.-F. Wang, C.M. Barrera, E.A. Dauer, W. Gu, F. Andreopoulos, C.-Y.C. Huang, Systematic characterization of porosity and mass transport and mechanical properties of porous polyurethane scaffolds. *J. Mech. Behav. Biomed.* 65 (2017) 657-664.
- [11] K.M. Sajesh, R. Jayakumar, S.V. Nair, K.P. Chennazhi, Biocompatible conducting chitosan/polypyrrole–alginate composite scaffold for bone tissue engineering. *Int. J. Biol. Macromol.* 62 (2013) 465-471.
- [12] A.M. Martins, J.D. Kretlow, A.R. Costa-Pinto, P.B. Malafaya, E.M. Fernandes, N.M. Neves, C.M. Alves, et al., Gradual pore formation in natural origin scaffolds throughout subcutaneous implantation. *J. Biomed. Mater. Res.* 100 (2012) 599-612.
- [13] A. Narmani, M. Rezvani, B. Farhood, P. Darkhor, J. Mohammadnejad, B. Amini, S. Refahi, et al., Folic acid functionalized nanoparticles as pharmaceutical carriers in drug delivery systems. *Drug Dev. Res.* 80 (2019) 404-424.
- [14] C. Cha, S.R. Shin, N. Annabi, M.R. Dokmeci, A. Khademhosseini, Carbon-based nanomaterials: multifunctional materials for biomedical engineering. *ACS Nano* 7 (2013) 2891-2897.
- [15] M.D. Dozois, L.C. Bahlmann, Y. Zilberman, X. (Shirley)Tan, Carbon nanomaterial-enhanced scaffolds for the creation of cardiac tissue constructs: A new frontier in cardiac tissue engineering. *Carbon* 120 (2017) 338-349.
- [16] J.-P. Salvetat, G.A.D. Briggs, J.-M. Bonard, R.R. Bacsa, A.J. Kulik, T. Stöckli, N. Burnham, et al., Elastic and shear moduli of single-walled carbon nanotube ropes. *Phys. Rev. Lett.* 82 (1999) 944-947.
- [17] L. Wang, Y. Wu, T. Hu, B. Guo, P.X. Ma, Electrospun conductive nanofibrous scaffolds for engineering cardiac tissue and 3D bioactuators. *Acta Biomaterialia* 59 (2017) 68-81.

- [18] S. Morimune, M. Kotera, T. Nishino, K. Goto, Katsuhiko Hata, Poly(vinyl alcohol) Nanocomposites with Nanodiamond. *Macromolecules* 44 (2011) 4415-4421.
- [19] C. Huang, N.L. Thomas, Fabricating porous poly(lactic acid) fibers via electrospinning. *Euro. Poly. J.* 99 (2018) 464-476.
- [20] A. Singh, A. Singh, D. Sen, Mesenchymal stem cells in cardiac regeneration: a detailed progress report of the last 6 years (2010-2015). *Stem Cell Res. Ther.* 7 (2016) 82.
- [21] L. Sensebe, P. Bourin, Mesenchymal stem cells for therapeutic purposes. *Transplantation* 87 (2009) 49-53.
- [22] A.M. Martins, G. Eng, S.G. Caridade, J.F. Mano, R.L. Reis, G.V. Novakovic, Electrically conductive chitosan/carbon scaffolds for cardiac tissue engineering. *Biomacromolecules* 15 (2014) 635-643.
- [23] A.M. Martins, C.M. Alves, F.K. Kasper, A.G. Mikos, R.L. Reis, Responsive and in situ-forming chitosan scaffolds for bone tissue engineering applications: an overview of the last decade. *J. Mater. Chem.* 20 (2010) 1638-1645.
- [24] G. Vozzi, C. Corallo, C. Daraio, Pressure-activated microsyringe composite scaffold of poly(L-lactic acid) and carbon nanotubes for bone tissue engineering. *J. Appl. Polym. Sci.* 129 (2013) 528-536.
- [25] F. Aubert-Viard, A. Martin, F. Chai, C. Neut, N. Tabary, B. Martel, N. Blanchemain, Chitosan finishing nonwoven textiles loaded with silver and iodide for antibacterial wound dressing applications. *Biomed. Mater.* 10 (2015) 015023.
- [26] Z. Abdeen Somaia, G. Mohammad, M.S. Mahmoud, Adsorption of Mn (II) ion on polyvinyl alcohol/chitosan dry blending from aqueous solution. *Environmental nanotechnology monitoring and management* 3 (2015) 1-9.

- [27] A.M. Smits, P.V. Vliet, C.H. Metz, T. Korfage, J.P.G. Sluijter, P.A. Doevendans, M.J. Goumans, Human cardiomyocyte progenitor cells differentiate into functional mature cardiomyocytes: an in vitro model for studying human cardiac physiology and pathophysiology. *Nat. Protoc.* 4 (2009) 232-243.
- [28] A. Narmani, J. Mohammadnejad, K. Yavari, Synthesis and evaluation of polyethylene glycol- and folic acid-conjugated polyamidoamine G4 dendrimer as nanocarrier. *J. Drug Deliv. Sci. Technol.* 50 (2019) 278-286.
- [29] S. Pok, F. Vitale, S.L. Eichmann, O.M. Benavides, M. Pasquali, J.G. Jacot, Biocompatible carbon nanotube–chitosan scaffold matching the electrical conductivity of the heart. *ACS Nano* 8 (2014) 9822-9832.
- [30] A. Narmani, K. Yavari, J. Mohammadnejad, Imaging, biodistribution and in vitro study of smart ^{99m}Tc -PAMAM G4 dendrimer as novel nano-complex. *Colloids Surf. B* 159 (2017) 232-240.
- [31] A. Narmani, M. Kamali, B. Amini, A. Salimi, Y. Panahi, Targeting delivery of oxaliplatin with smart PEG-modified PAMAM G4 to colorectal cell line: *In vitro* studies. *Process Biochemistry* 69 (2018) 178-187.
- [32] B.A.Baker, P.S. Pine, K. Chatterjee, G. Kumar, N.J. Lin, J.H. McDaniel, et al., Ontology analysis of global gene expression differences of human bone marrow stromal cells cultured on 3D scaffolds or 2D films. *Biomaterials* 35 (2014) 6716-6726.
- [33] S.F. Wang, L. Shen, W.D. Zhang, Y.J. Tong, Preparation and mechanical properties of chitosan/carbon nanotubes composites. *Biomacromolecules* 6 (2005) 3067-3072.
- [34] A. Larrañaga, A. Alonso-Varona, T. Palomares, E. Rubio-Azpeitia, P. Aldazabal, F.J. Martin, J.R. Sarasua, Effect of bioactive glass particles on osteogenic differentiation of

adipose-derived mesenchymal stem cells seeded on lactide and caprolactone based scaffolds. *J Biomed Mater Res A* 103 (2015) 3815-3824.

[35] S. Halelfadl, P. Estellé, B. Aladag, N. Doner, T. Maré, Viscosity of carbon nanotubes water-based nanofluids: Influence of concentration and temperature. *Int. J. Therm. Sci.* 71 (2013) 111-117.

[36] Y. Zare, K. Yop Rhee, A simple model for electrical conductivity of polymer carbon nanotubes nanocomposites assuming the filler properties, interphase dimension, network level, interfacial tension and tunneling distance. *Compos. Sci. Technol.* 155 (2018) 252-260.

[37] X. Zhao, P. Li, B. Guo, P.X. Ma, Antibacterial and conductive injectable hydrogels based on quaternized chitosan-graft-polyaniline/oxidized dextran for tissue engineering. *Acta Biomaterialia* 26 (2015) 236-248.

[38] S.D. McCullen, D.R. Stevens, W.A. Roberts, S.S. Ojha, L.I. Clarke, R.E. Gorga, Morphological, electrical, and mechanical characterization of electrospun nanofiber mats containing multiwalled carbon nanotubes. *Macromolecules* 40 (2007) 997-1003.

[39] P. Szatkowski, K. Pielichowska, S. Blazewicz, Mechanical and thermal properties of carbon-nanotubereinforced self-healing polyurethanes. *J. Mater. Sci.* 52 (2017) 12221-12234.

[40] X. Zhao, B. Guo, H. Wu, Y. Liang, P.X. Ma, Injectable antibacterial conductive nanocomposite cryogels with rapid shape recovery for noncompressible hemorrhage and wound healing. *Nat. Commun.* 9 (2018) 2784.

[41] E.A. Naumenko, I.D. Guryanov, R. Yendluri, Y.M. Lvov, R.F. Fakhrullin, Clay nanotube-biopolymer composite scaffolds for tissue engineering. *Nanoscale* 8 (2016) 7257-7271.

[42] C.L. Ursini, R. Maiello, A. Ciervo, A.M. Freseigna, G. Buresti, F. Superti, M. Marchetti, et al., Evaluation of uptake, cytotoxicity and inflammatory effects in respiratory cells exposed to

pristine and –OH and –COOH functionalized multi-wall carbon nanotubes. *J. Appl. Toxicol.* 36 (2015) 394-403.

[43] M. Rezvani, J. Mohammadnejad, A. Narmani, K. Bidaki, Synthesis and in vitro study of modified chitosan-polycaprolactam nanocomplex as delivery system. *Int. J. Biol. Macromol.* 113 (2018) 1287-1293.

[44] M.C. Serrano, M.C. Gutiérrez, F. Monte, Role of polymers in the design of 3D carbon nanotube-based scaffolds for biomedical applications. *Prog. Polym. Sci.* 39 (2014) 1448-1471.

[45] Y. Zhang, Y. Yu, F. Dolati, I.T. Ozbolat, Effect of multiwall carbon nanotube reinforcement on coaxially extruded cellular vascular conduits. *Mater. Sci. Eng. C.* 39 (2014) 126-133.

[46] S. Wang, X. Gao, W. Gong, Z. Zhang, X. Chen, Y. Dong, Odontogenic differentiation and dentin formation of dental pulp cells under nanobioactive glass induction. *Acta biomaterialia* 10 (2014) 2792-2803.

[47] S.J. Xu, Z.Y. Qiu, J.J. Wu, X.D. Kong, X.S. Weng, F.Z. Cui, X.M. Wang, Osteogenic differentiation gene expression profiling of hMSCs on hydroxyapatite and mineralized collagen. *Tissue Eng. A* 22 (2016) 170-181.